SIMULATION OF ROTATIONAL DIFFUSION AND HYDRATION OF LAURDAN IN A DPPC BILAYER

by

Ryan Frei

A senior thesis submitted to the faculty of

Brigham Young University

in partial fulfillment of the requirements for the degree of

Bachelor of Science

Department of Physics and Astronomy

Brigham Young University

April 2007

Copyright © 2007 Ryan Frei

All Rights Reserved

BRIGHAM YOUNG UNIVERSITY

DEPARTMENT APPROVAL

of a senior thesis submitted by

Ryan Frei

This thesis has been reviewed by the research advisor, research coordinator, and department chair and has been found to be satisfactory.

Date	Gus Hart, Advisor
Date	Eric Hintz, Research Coordinator
Date	Scott D. Sommerfeldt, Chair

ABSTRACT

SIMULATION OF ROTATIONAL DIFFUSION AND HYDRATION OF LAURDAN IN A DPPC BILAYER

Ryan Frei

Department of Physics and Astronomy

Bachelor of Science

We have used molecular dynamics simulations to investigate the rotational diffusion and hydration of Laurdan (2-dimethylamino-6-lauroylnaphthalene) in liquid and gel dipalmitoylphosphatidylcholine bilayers at temperatures above and below the phase transition. Laurdan is a fluorescent dye commonly used in biophysical experiments to detect ordered regions in lipid bilayers through changes in the polarization and wavelength of emitted light. Correlation between the autocorrelation of the laurdan rotation and experimental observations of the decay of anisotropy of the emitted light and between hydration and shift in fluorescence wavelengths is demonstrated.

ACKNOWLEDGMENTS

I would like to thank Dr. David Busath for his guidance. Also I would like to acknowledge the Ira and Marylou Fulton Supercomputing center at Brigham Young University and the Brigham Young University mentoring grants for support.

Contents

List of Figures

Chapter 1

Introduction

1.1 Bilayer order and lipid rafts

Cell membranes are made up of lipid bilayers, with the hydrophobic tails of the lipids on the inside and the hydrophilic headgroups on the outside. Lipid bilayers have some very interesting properties, such as two-dimensional fluidity and complex phase properties. Lipid rafts are areas of bilayers where there is higher order than in the surrounding lipids [1]. The order or disorder of the bilayer at a given temperature depends on the temperature and the presence of rigid molecules such as cholesterol and sphingolipids [2]. In cell membranes, areas of higher order and higher cholesterol and sphingolipid concentration form spontaneously. It is thought that these regions of higher order are made energetically favorable by intermolecular van der Waals interactions [3]. This type of formation is an intrinsic property of lipid bilayers, as has been demonstrated by the fact that they form not only in cell membranes, but also in model bilayers [4].

Several theories have been formulated surrounding the purpose of lipid rafts, but the most commonly cited is the theory proposed by Kai Simons [5, 6]. In this theory

they are thought to be relatively small structures (about 50 nm) associated with intracellular trafficking [3] and intercellular signaling mechanisms [7]. Understanding the dynamical function of these rafts can help us to better understand these processes.

The phospholipid dipalmitoylphosphotidylchoine (DPPC) undergoes a transition from the solid-ordered phase to the liquid-disordered phase at approximately 41.5°C [8]. In the liquid phase, two distinct subphases exist in lipid bilayers: liquid ordered and liquid disordered, based on the densities of such rigid molecules as cholesterol and sphingolipids. The principle difference between these phases is in the order of the lipid tails; hence, they are referred to a liquid-ordered and liquid-disordered.

1.2 Raft detection

The biochemical method used to detect rafts involves dissolving the bilayers with strong detergents and collecting the remaining particles. The rafts in the bilayers resist the detergents, remaining intact as larger particles. While this method is useful in analysis of raft composition, the destruction of the bilayer makes any analysis of the rafts' function impossible. Also, this approach is fraught with questions as to whether the rafts existed in the membranes before the detergents or if they are a result of, or are at least modified by, the dissolving process. Similarly, removal or addition of cholesterol, with β-cyclodextrin [9] for example, has been useful for assessing the role of rafts in membrane protein function [5, 9, 10].

Another method of raft detection, developed by Parasassi *et al.* for detecting ordered regions in bilayers, is the use of fluorescent dyes [11]. Dyes are injected into the bilayer, and the fluorescent emissions change with the order of the bilayer. Injecting dyes has the obvious advantage of being nondestructive to the bilayer, and also allows high-resolution imaging of bilayers. In recent studies, these dyes have even

enabled imaging of the membranes of human erythrocytes [12].

1.3 The mechanism of fluorescence spectroscopy

The two fluorescence-spectroscopic methods commonly used in lipid phase detection are the generalized polarization (GP) and the polarization anisotropy (PA) of emitted light. GP is based on a shift in the wavelength of the emission spectrum. PA is based on analysis of the uniformity of emission polarization when a polarized source is used.

Several different dyes are used in fluorescence spectroscopy, including laurdan, prodan, and 1,6-diphenyl-1,3,5-hexatriene. These dyes partition into varying depths of the bilayer, making them useful for measuring different bilayer properties. Of the three mentioned, laurdan is the most widely used, and hence is the subject of our study. A schematic diagram of the laurdan structure is shown in Fig. 1.1.

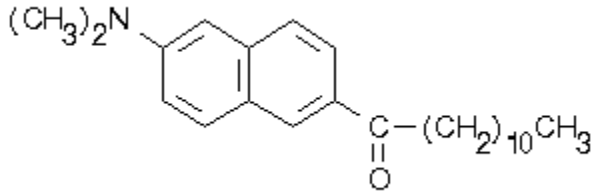

Figure 1.1 A schematic diagram of laurdan, a fluorescent dye commonly used in fluorescence spectroscopy.

1.3.1 Generalized polarization

The GP is a measure of how far the emission spectrum of the dye shifts from the absorption and is calculated as

$$GP = \frac{I_B - I_R}{I_B + I_R} \tag{1.1}$$

where I_B and I_R are the emission intensities at the blue and red edges of the emission spectrum [11]. It is thought that GP is influenced by the mobility of polar solvent molecules surrounding the π-cloud of the naphthalene group, which partitions into the headgroup region. This means that the packing of the lipid headgroups is a primary factor in the laurdan GP.

The lower panel of Fig. 1.2 shows a normalized plot of the GP with a calorimetric phase diagram overlaid. The regions where the GP changes correspond with the theoretical phase changes. This correspondence makes analysis of GP very useful in distinguishing between the liquid-disordered phase and other phases. The order of the lipid tails has almost no impact on the GP, which means that it cannot detect the differences between the liquid-ordered and solid-ordered phases.

1.3.2 Polarization anisotropy

Harris *et al.* showed that the PA of fluorescence emissions can also be used to detect the order of bilayers [13]. The dependence on tail order gives a significant difference between the liquid-ordered phase and the solid-ordered phase. In the top panel of Fig. 1.2, the PA of laurdan in a DPPC bilayer is shown with a calorimetric phase diagram overlaid in red. This figure illustrates the usefulness of laurdan in detecting differences between the solid-ordered and liquid-ordered phases. Although GP and PA are both limited in the phase transitions they can image, in combination they give a relatively complete picture of the phase diagram for a bilayer.

1.4 Simulations of dyes in bilayers

Molecular dynamics simulations provide a way to investigate the mechanisms of such complex phenomena as the sources of the PA imaging. Some of the difficulties of

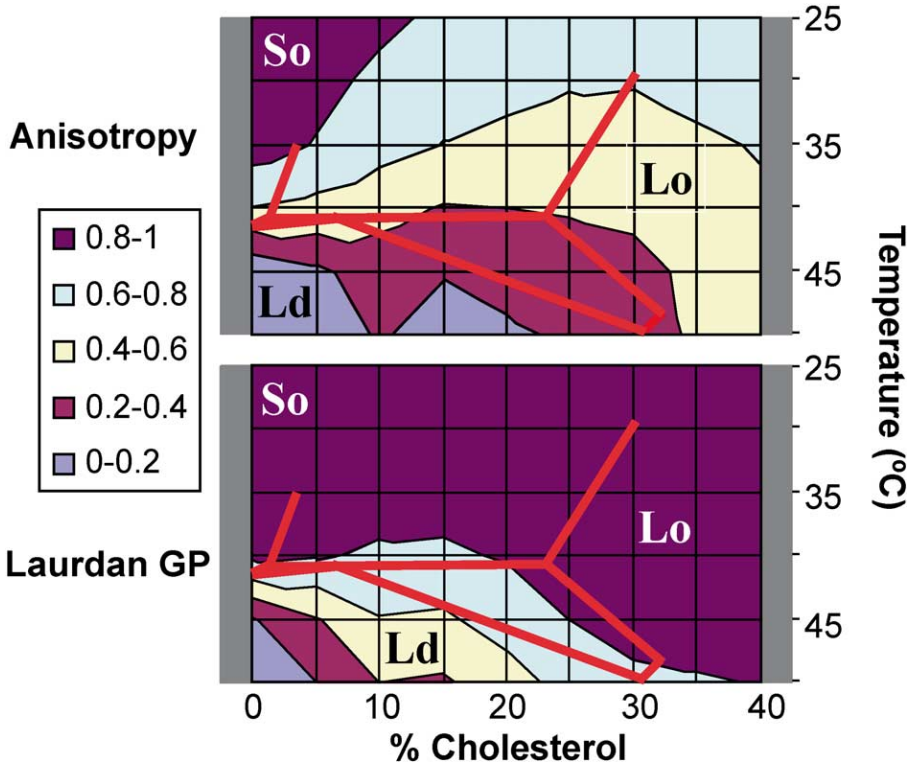

Figure 1.2 Laurdan GP and PA. A calorimetric phase diagram of DPPC and cholesterol mixtures is overlaid in red lines and the phases of various regions are labeled. Normalized values of PA (upper panel) and GP (lower panel) corresponding to the different colors are shown in the legend on the figure. The phase diagram (red lines) is based on Ref. [2]. 'So' indicates the solid ordered phase, 'Lo' liquid ordered phase, 'Ld' liquid disordered phase. From Harris *et al.*, 2002 [13]. Used with permission.

doing molecular dynamics simulations of complex structures such as bilayers include choosing the right volume for the periodic box that encloses the bilayer and choosing the correct surface tension.

The peak emission wavelength shift in GP is thought to be due to mobility of polar solvent molecules, which is related to headgroup spacing. GP, being a primarily quantum mechanical effect, is difficult to investigate rigorously using classical techniques. However, we are able to show how hydration, or the number of water molecules near a laurdan molecule, relates to temperature and order of the bilayer.

The changes in PA are thought to be related to the fluidity of the bilayers. Since this is a completely classical phenomenon, it lends itself quite readily to analysis with molecular dynamics simulations.

The mechanism of both of these phenomena is not fully understood. We have used classical molecular dynamics simulations to investigate the mechanisms of both GP and PA.

We performed simulations of laurdan in a DPPC bilayer using the Nanoscale Molecular Dynamics (NAMD) simulator developed by the Theoretical and Computational Biophysics Group in the Beckman Institute for Advanced Science and Technology at the University of Illinois at Urbana-Champaign [14]. We did this with the intent of comparing our results to known experimental values of GP and PA.

Chapter 2

Computational methods

2.1 Bilayer Arrangement

We simulated a model bilayer with 5x5 DPPC molecules in each monolayer in the central cell. We deleted the central molecule of each monolayer and inserted a laurdan molecule into its place. The entire bilayer was surrounded in the simulation by 1440 water molecules initially equally partitioned on both sides of the molecule The arrangement of the system is shown in Fig. 2.1.

At our periodic cell boundaries we used a cutoff of 12.0Å in calculating the direct electrostatic and van der Waals interactions. To calculate the long-range interactions of the bilayer, we used a fifth-order particle-mesh Ewalds algorithm, which computes the long-range effects of the periodic cell in the reciprocal space.

2.2 Dynamics Simulation

The protocol used in our dynamic simulation consisted of an energy minimization, a short equilibration at 323 K, an annealing phase described later, a longer equilibra-

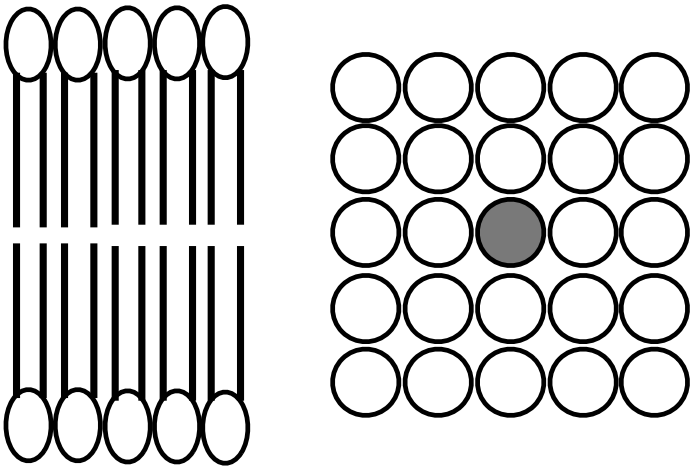

Figure 2.1 A schematic diagram of the system arrangement. The left panel shows a side view of the system, with the headgroups of the lipids shown as circles with the tails extending from them. The right panel shows a top view with the laurdan molecule shaded.

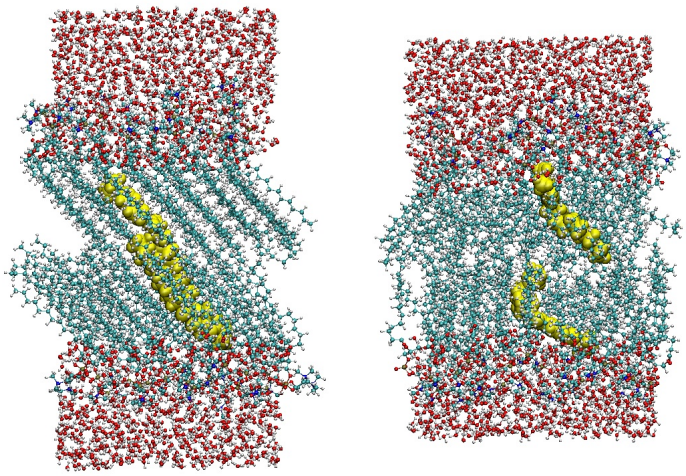

Figure 2.2 A typical output of our system after minimization, annealing, and a 10 ns equilibration. The figure on the left is the system simulated at $T = 20°\mathrm{C}$ and the one on the right is simulated at $T = 50°\mathrm{C}$. The yellow molecules are laurdan in their typical conformation. Note the slant of the lipid tails and the highly ordered crystal structure of the solid ordered phase ($T = 20°\mathrm{C}$ system, and the disorder of the tails of the system in the liquid disordered phase ($T = 50°\mathrm{C}$).

tion at the target temperatures of 293 K and 323 K, followed by 20 ns of dynamics simulation holding the normal pressure, surface tension, and temperature constant.

A summary of the algorithm is shown in Table 2.1. In the annealing phase of the simulation, we simulated heating the system to 1000 K for 500 ps and then allowed it to cool to the final temperature for 1 ns. This process was repeated three times. In the simulation stage, we started four different simulations after the last equilibration, in an effort to create a larger statistical sample.

During the equilibration and annealing stages, a 5 dyne/cm harmonic planar constraining force was used on the lipid phosphorous atoms. This was done to allow the proper level of disorder to develop in the tails of the lipids for the experimentally determined membrane thicknesses. During the simulation, a 0.1 dyne/cm harmonic cylindrical constraining force was applied to the laurdan molecule to keep it in the center of the periodic cell. A typical results of this simulation is illustrated in Fig. 2.2.

2.3 Surface tension

There is general agreement among those simulating lipid bilayers that in order to have a bilayer that has correct thickness and surface area per headgroup, an external surface tension must be applied [15–26]. The reason for this has been explained by Feller *et al.* [18] as a result of the simulated bilayer's lack of periodic undulations and other structural features present in macroscopic bilayers.

We determined the target surface tension needed in this system by simulating several different systems with varying surface tensions and analyzing the surface area per lipid headgroup, which was targeted to experimental values. This is the variable most affected by varying surface tensions. The area per lipid headgroup has been measured using several different methods, and it is known within ±9%. A good

Stage	**Time**	**Ensemble**	**Constraints**
Minimization	5000 steps	None	None
Heating	500 ps	NP	5 dyne/cm on lipids
Equilibration	1 ns	NP	5 dyne/cm on lipids
Annealing	4.5 ns	NV	5 dyne/cm on lipids
Equilibration	10 ns	$NP\gamma T$	5 dyne/cm on lipids
Simulation	20 ns	$NP\gamma T$	0.1 dyne/cm on laurdan

Table 2.1 The dynamics simulation algorithm used in this system. The Ensemble column indicates which variables were held constant in that stage of simulation. The abbreviations used are as follows: N, number; P, pressure; V, volume; γ, surface tension; and T, temperature. The constraints on the lipids were planar, holding the bilayer to experimentally determined thicknesses. The constraints on the laurdan molecule were cylindrical, holding it in the center of the bilayer, helping to reduce the effects of using a finite periodic cell.

discussion of this structural parameter can be found in Refs. [27] and [28].

The primary difficulty of this approach is not knowing the area occupied by the laurdan molecule. Approximating it to be about the size of a lipid, we can get within ±5% of the actual area per headgroup, which is about the size of the thermal fluctuations of the simulation and about half the uncertainty in the experimental surface area. Using this method, we determined that a surface tension of about 25 dyne/cm gives results in agreement with experimental surface areas per headgroup. This is close to surface tensions given by published simulation results [21, 22].

2.4 Analysis

There were two major computational components to our analysis. We analyzed the hydration of the laurdan to investigate the correlation between this hydration and the generalized polarization. We also analyzed the autocorrelation function of the laurdan axial vector and used it to calculate the polarization anisotropy of the molecule.

To analyze the hydration of the laurdan molecules, we counted water molecules inside the headgroup region and within a certain distance of the laurdan molecule. To analyze the autocorrelation of the orientation of the laurdan we defined a vector passing through the carbonyl C and amino N of the laurdan as $\vec{S}$. The correlation function is determined by taking the ensemble time average of two vectors. Autocorrelation is found by taking the time average of the dot product of a vector with itself at a different time:

$$A(\tau) = \left\langle \vec{S}(t) \cdot \vec{S}(t+\tau) \right\rangle_t . \tag{2.1}$$

For a randomly varying function, Eq. 2.1 will yield a roughly exponential decay to zero. The characteristic fluorescence-emission time of the laurdan was used together with the decay time constant to calculate the polarization anisotropy predicted by

our simulations.

Chapter 3

Results and Discussion

Analysis of the simulations of laurdan in a DPPC bilayer yields two quantities which lend themselves to comparison with experimental values – the hydration of the laurdan molecule and the rotational autocorrelation function. The hydration, which is related to the lipid headgroup spacing and the generalized polarization can be analyzed qualitatively, which yields a qualitative correlation with the GP. Rotational autocorrelation, which is related to the rate of rotation and hence is related to the polarization anisotropy, gives a much more quantitative comparison to experimental data.

3.1 Hydration

In order to analyze the hydration of the laurdan molecule, we performed a simulation of laurdan dissolved in bulk water. A count of the number of water molecules near the laurdan in DPPC divided by a similar count in bulk water gives us a feel of the reduction by DPPC of the quantity of water surrounding laurdan. The ratio of the hydration of laurdan in a bilayer to the hydration in bulk water is shown in Fig. 3.1.

As can be seen in the plot, the region closer to the laurdan is significantly more hydrated in the 50°C simulation.

The region within 5 Å of the laurdan molecule has a statistically significant difference in hydration between the 20°C and 50°C simulations. The average over the 20 ns simulation this region has an average of 11.8 molecules in the 20°C simulation and 13.3 in the 50°C simulation. For this relationship to be more quantitative, a thorough quantum mechanical analysis would have to be performed. However, it may be useful in the future to establish a qualitative correlation of hydration with temperature for comparison to experimental GP.

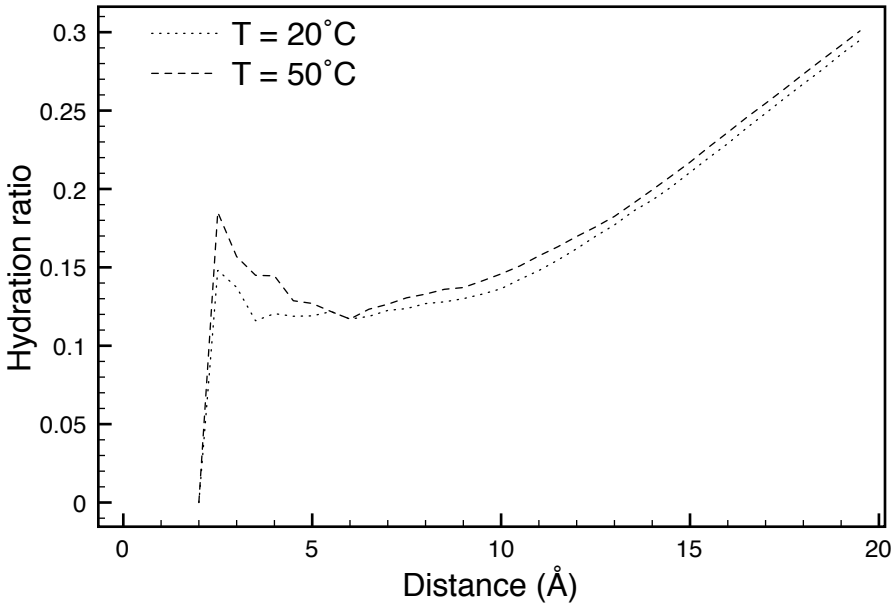

Figure 3.1 The ratio of the radial distribution function for water oxygen atoms near any laurdan atom in DPPC to that in bulk water. The region with the statistically significant difference in that between 0 Å and 5 Å. In this range there is an average of 11.8 molecules in the 20°C simulation and 13.3 in the 50°C simulation.

3.2 Rotational diffusion

The autocorrelation function for the laurdan molecule, averaged for two molecules over two separate 20 ns runs, is shown in Fig. 3.2. From this figure, it is clear that the rate of rotational diffusion at 50°C is much higher than that at 20°C. This fits with experimental anisotropy measurements. Fitting these curves to a decaying exponential, we get a characteristic decay time of 96.2 ns at 20°C, and 8.3 ns at 50°C. The characteristic rate of rotation of a laurdan molecule in a bilayer is related to the anisotropy by the equation:

$$T = \frac{6t}{(r_0/r) - 1}, \tag{3.1}$$

where T is the average rotational period, t is the average lifetime of laurdan fluorescence, r is the measured anisotropy, and r_0 is the maximum anisotropy [13]. We can use the measurement of Harris *et al.* of 0.26 as the lowest maximum anisotropy and the theoretical value of 0.44 as the highest maximum anisotropy. Using this in Eq. 3.1, we can conclude that for our system that the average rotational period T at 50°C should be 6.7-13.3 ns and for 20°C it should be greater than 71.4 ns. The characteristic time of the autocorrelation of the laurdan orientation measured in our system falls within these ranges.

3.3 Conclusions

The theoretical mechanism of the GP is that polar solvent molecules near an excited fluorophore bleed some electron energy, reducing the energy of the eventual photon emitted [11,29]. The increased hydration at 50°C illustrates this mechanism. In order to explore the relationship of hydration and GP, simulations at varying temperatures and cholesterol concentrations could be helpful, although a full analysis would require a quantum-mechanical model of energy transfer to solvent molecules.

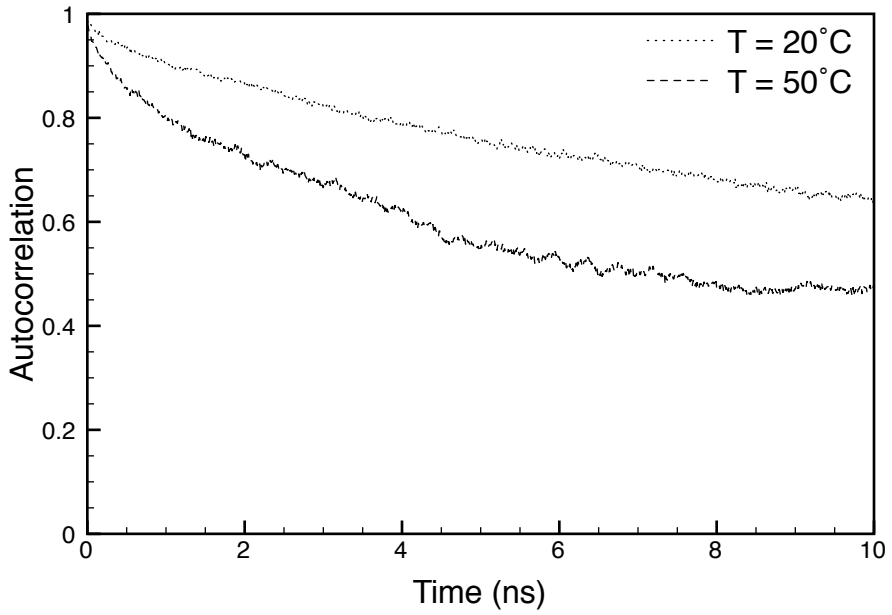

Figure 3.2 The autocorrelation of the laurdan axial vector. The characteristic decay time of the 20°C is 96.2 ns and of the 50°C is 8.3 ns.

PA is theorized to stem from fluorophore rotation between excitation and emission [13], and would be increased by increased mobility of the lipid molecules. The autocorrelation relaxation of simulated laurdan molecules corresponds well with experimentally established values of polarization anisotropy. It would be interesting in the future to carry out a more complete analysis of the effects of added cholesterol, which is known to modulate PA [13].

These simulations pave the way for future studies of the impact of cholesterol or other reagents added to the bilayer, of lipid species, and of lipid phase on fluorophore properties, as well as for detailed studies of other probes such as prodan or 1,6-diphenyl-1,3,5-hexatriene, which in preliminary simulations partition shallower or deeper, respectively, into the bilayer.

Bibliography

[1] A. Rietveld and K. Simons, "The differential miscibility of lipids as the basis for the formation of functional membrane rafts," Biochimica et Biophysica Acta **1376,** 467–479 (1998).

[2] J. L. Thewalt and M. Bloom, "Phosphatidylcholine: cholesterol phase diagrams," Biophysical Journal **63,** 1176–1181 (1992).

[3] J. B. Helms and C. Zurzolo, "Lipids as Targeting Signals: Lipid Rafts and Intracellular Trafficking," Traffic **5,** 247–254 (2004).

[4] C. Dietrich, L. A. Bagatolli, Z. N. Volovyk, N. L. Thompson, M. Levi, K. Jacobson, and E. Gratton, "Lipid Rafts Reconstituted in Model Membranes," Biophysical Journal **80,** 1417–1428 (2001).

[5] K. Simons and E. Ikonen, "Functional rafts in cell membranes," Nature **387,** 569–572 (1997).

[6] A. Pralle, P. Keller, E.-L. Florin, K. Simons, and J. Hörber, "Sphingolipid–Cholesterol Rafts Diffuse as Small Entities in the Plasma Membrane of Mammalian Cells," Journal of Cell Biology **148,** 997–1007 (2000).

[7] K. Simons and D. Toomre, "Lipid rafts and signal transduction," Mol. Cell Biol. **1,** 31–41 (2000).

[8] N. Albon and J. M. Sturtevant, "Nature of the Gel to Liquid Crystal Transition of Synthetic Phosphatidylcholines," Proc. Natl. Acad. Sci. **75,** 2258–2260 (1978).

[9] B. U. Samuel, N. Mohandas, T. Harrison, H. McManus, W. Rosse, M. Reid, and K. Haldar, "The Role of Cholesterol and Glycosylphosphatidylinositol-anchored Proteins of Erythrocyte Rafts in Regulating Raft Protein Content and Malarial Infection," Journal of Biological Chemistry **276,** 29319–29329 (2001).

[10] A. G. Ostermeyer, B. T. Beckrich, K. A. Ivarson, K. E. Grove, and D. A. Brown, "Glycosphingolipids Are Not Essential for Formation of Detergent-resistant Membrane Rafts in Melanoma Cells," Journal of Biological Chemistry **274,** 34459–34466 (1999).

[11] T. Parasassi, G. D. Stasio, G. Ravagnan, R. M. Rusch, and E. Gratton, "Quantitation of lipid phases in phospholipid vesicles by the generalized polarization of Laurdan fluorescence," Biophysical Journal **60,** 179–189 (1991).

[12] R. Vest, R. Wallis, L. B. Jensen, A. C. Haws, J. Callister, B. Brimhall, A. M. Judd, and J. D. Bell, "Use of Steady-State Laurdan Fluorescence to Detect Changes in Liquid Ordered Phases in Human Erythrocyte Membranes," Journal of Membrane Biology **211,** 15–25 (2006).

[13] F. M. Harris, K. B. Best, and J. D. Bell, "Use of laurdan fluorescence intensity and polarization to distinguish between changes in membrane fluidity and phospholipid order," Biochimica et Biophysica Acta **1565,** 123–138 (2002).

[14] J. C. Phillips, R. Braun, W. Wang, J. Gumbart, E. Tajkhorshid, E. Villa, C. Chipot, R. D. Skeel, L. Kale, and K. Schulten, "Scalable molecular dynamics with NAMD," Journal of Computational Chemistry **26,** 1781–1802 (2005).

[15] S.-W. Chiu, M. Clark, V. Balaji, S. Subramaniam, H. L. Scott, and E. Jakobsson, "Incorporation of Surface Tension into Molecular Dynamics Simulation of an Interface: A Fluid Phase Lipid Bilayer Membrane," Biophysical Journal **69,** 1230–1245 (1995).

[16] S. E. Feller, Y. Zhang, and R. W. Pastor, "Computer simulation of liquid/liquid interfaces. II. Surface tension-area dependence of a bilayer and monolayer," J. Chem. Phys. **103,** 10267–10276 (1995).

[17] C. Tapia-Medina, P. Orea, L. Mier-y Teran, and J. Alejandre, "Surface tension of associating fluids by Monte Carlo simulations," J. Chem. Phys. **120,** 2337–2342 (2004).

[18] S. E. Feller and R. W. Pastor, "On Simulating Lipid Bilayers with an Applied Surface Tension: Periodic Boundary Conditions and Undulations," Biophysical Journal **71,** 1350–1355 (1996).

[19] S. E. Feller, R. W. Pastor, A. Rojnuckarin, S. Bogusz, and B. R. Brooks, "Effect of Electrostatic Force Truncation on Interfacial and Transport Properties of Water," J. Chem. Phys. **100,** 10711–17020 (1996).

[20] S. E. Feller and R. W. Pastor, "Length scales of lipid dynamics and moleuclar dynamics," Pac Symp Biocomput. pp. 142–150 (1997).

[21] S. E. Feller and R. W. Pastor, "Constant surface tension simulations of lipid bilayers: The sensitivity of surface areas and compressibilities," J. Chem. Phys. **111,** 1281–1287 (1999).

[22] R. Sankararamakrishnan and H. Weinstein, "Surface Tension Parameterization in Molecular Dynamics Simulations of a Phospholipid-bilayer Membrane: Calibration and Effects," J. Phys. Chem. B **108,** 11802–11811 (2004).

[23] J. Stecki, "Correlations in simulated model bilayers," J. Chem. Phys. **120,** 3508–3516 (2004).

[24] A. H. de Vries, I. Chandrasekhar, W. F. van Gunsteren, and P. H. Hunenberger, "Molecular Dynamics Simulations of Phospholipid Bilayers: Influence of Artificial Periodicity, System Size, and Simulation Time," J. Phys. Chem. B **109,** 11643–11652 (2005).

[25] Y. Zhang, S. E. Feller, B. R. Brooks, and R. W. Pastor, "Computer simulation of liquid/liquid interfaces. I. Theory and application to octane/water," J. Chem. Phys. **103,** 10252–10266 (1995).

[26] Q. Zhu and M. W. Vaughn, "Surface Tension Effect on Transmembrane Channel Stability in a Model Membrane," J. Phys. Chem. B **109,** 19474–19483 (2005).

[27] J. F. Nagle and S. Tristram-Nagle, "Structure of lipid bilayers," Biochimica et Biophysica Acta **1469,** 159–195 (2000).

[28] S. Tristram-Nagle and J. F. Nagle, "Lipid bilayers: thermodynamics, structure, fluctuations, and interactions," Chem and Phys of Lipids **127,** 3–14 (2004).

[29] J. R. Lakowicz, *Principles of Fluorescence Spectroscopy* (Plenum Publishing Corp., New York, 1983).

Index